

Resistive Switching Phenomena in Li_xCoO_2 Thin Films

Alec Moradpour,* Olivier Schneegans, Sylvain Franger, Alexandre Revcolevschi, Raphaël Salot, Pascale Auban-Senzier, Claude Pasquier, Efthymios Svoukis, John Giapintzakis, Oana Dragos, Vasile-Cristian Ciomaga, and Pascal Chrétien

Although the initial studies of bipolar (polarity dependent) electrical resistive switching in thin-film MIM (metal/insulator/metal) devices date back to more than forty years ago,^[1] the most elaborate study in this area, proving experimentally the concept of memory resistors (memresistors), the resistance values of which depend on the electrical charge that had crossed them, was published only very recently.^[2] Subsequently, this newly reviewed topic^[3] is now being very actively investigated.^[4] In view of non-volatile memory applications (resistive random access memory (ReRAM)), and considering the mechanisms involved in the bipolar resistive switching phenomena, three systems related to chemical effects, among a variety of other physical effects, have been suggested:^[3] i) electrochemical metallization systems, relying on electrochemically active (sacrificial) metal electrodes such as Ag; ii) valence change systems, occurring in specific transition metal oxides and triggered by electromigration of anions (i.e., oxygen vacancies), which lead to a redox reaction involving the transition metal sublattice, and a subsequent change in conductivity; and iii) thermochemical

systems based on current-induced temperature-increase effects. Interestingly, it is a re-investigation of a Pt/TiO₂/Pt stack,^[1] belonging to the valence change systems, that led to the experimental substantiation of memresistors.^[2]

In this study, we have investigated conducting-probe atomic force microscopy (CP-AFM) modifications of polycrystalline Li_xCoO_2 thin films. We show that reversible local surface-conductivity changes are obtained within these samples. This led us to realize that the processes observed in these thin-film modifications, fully consistent with the previously examined conducting-probe mediated modifications of more ordered Na_xCoO_2 single crystals,^[5] evoke, in fact, the behavior of MIM stacks. Therefore, the observed phenomena may not be restricted to surface-conductivity modifications, but might reflect a possible resistive switching process involving these thin films. We first report the results for the CP-AFM mediated surface-conductivity modifications of Li_xCoO_2 thin films, and second show through the study of an MIM device (I stands for Li_xCoO_2) that resistive switching is observed, for the first time, in a layered alkali-metal intercalation-based mixed conductor thin-film.

The earlier Na_xCoO_2 probe-mediated reversible modifications^[5] illustrated a fine control over the surface conductivity of the single crystals: depending on the value and the polarization direction of the probe-to-sample applied potential, local control of the surface-conductivity of single crystals is possible, as shown in **Figure 1a**. Comparable surface-modifications (**Figure 1b**), mediated by CP-AFM operating now in ambient air, are also observed in the, more disordered, Li_xCoO_2 thin films grown either on highly doped silicon wafers by sputtering, or on sapphire single crystals by pulsed laser deposition (PLD). Thus, for positive (oxidative) modification-bias a more conductive area than the starting thin-film surface is observed, while a negative value of the modification bias yields the formation of an insulating region (images recorded at +1 V bias voltage). These surface modifications are reversible, similar to the previous surface modifications of Na_xCoO_2 single crystals. This is shown by the consecutive formation of conducting and insulating regions, formed in concentric square areas of decreasing size, when scanned using opposite probe potential polarities, as illustrated in **Figure 1c**. We have previously attributed^[5] the surface-conductivity modifications of Na_xCoO_2 to electrochemical reactions occurring within the condensation water capillary meniscus at the probe/substrate contact,^[6] and a similar electrochemical phenomenon may account for the present Li_xCoO_2 thin film modifications. These probe-mediated local processes may thus also involve redox reactions of the cobalt oxide sublattice, coupled to the simultaneous occurrence of lithium

Dr. A. Moradpour, Dr. P. Auban-Senzier, Prof. C. Pasquier
Laboratoire de Physique des Solides
UMR C8502 of CNRS
University Paris-Sud 11
91405 Orsay Cedex, France
E-mail: moradpour@lps.u-psud.fr

Dr. O. Schneegans, P. Chrétien
Laboratoire de Génie Electrique de Paris
UMR 8507 of CNRS
Paris VI and Paris-Sud Universities
Supélec, 91192 Gif-sur-Yvette Cedex, France

Dr. S. Franger, Prof. A. Revcolevschi, Dr. O. Dragos,^[+] V.-C. Ciomaga
Institut de Chimie Moléculaire et des Matériaux d'Orsay
Laboratoire de Physico-Chimie de l'Etat Solide
UMR 8182 of CNRS
University Paris-Sud
91405 Orsay Cedex, France

Dr. R. Salot
CEA/LITEN
17 Avenue des Martyrs
38054 Grenoble Cedex 09, France
E. Svoukis, Prof. J. Giapintzakis
Department of Mechanical and Manufacturing Engineering
University of Cyprus
75 Kallipoleos Avenue
PO Box 20537, 1678 Nicosia, Cyprus

[+] Present address: Nat. Inst. R&D Tech. Phys., 47 Mangeron Ave.,
700050, Iasi, Romania

DOI: 10.1002/adma.201101800

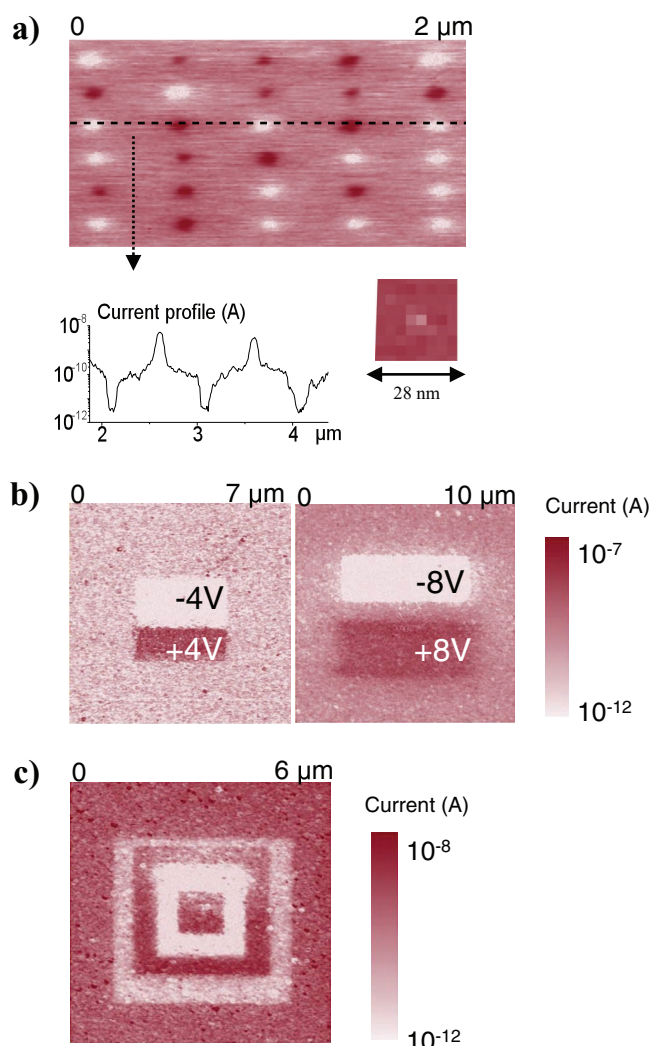


Figure 1. CP-AFM mediated surface-conductivity modifications of Na_xCoO_2 single crystals and of Li_xCoO_2 thin films, recorded at +1 V; a) more conducting and more insulating (than the native surface) spots obtained on a freshly cleaved Na_xCoO_2 single crystal *ab* face (under nitrogen atmosphere), using (5 ms) +4 and -3 V bias pulses. The lowest spot size (≈ 7 nm) reachable with our present pulse time (0.1 ms) is shown on the lower right corner; b) more conducting areas (dark red rectangles) than the initial surfaces are obtained by scanning (in ambient air) Li_xCoO_2 films with sample/tip anodic biases (+4 and +8 V for thin films obtained respectively by PLD and radio frequency (RF) sputtering); opposite biases (-4 and -8 V) lead to more insulating rectangular regions; c) concentric squares decreasing in size are obtained on an Li_xCoO_2 thin film surface (RF sputtering), showing the reversibility of the process: an initial $4 \times 4 \mu\text{m}^2$ scan with a -4 V sample-tip bias yields a more insulating region, a second scan ($3 \times 3 \mu\text{m}^2$ at +4 V) yields back a more conducting region, and further scans ($2 \times 2 \mu\text{m}^2$ at -4 V, and then $1 \times 1 \mu\text{m}^2$ at +2.5 V) lead successively to a more insulating and finally a more conducting central area.

ion intercalation/deintercalation steps as required by electro-neutrality, to control the electronic properties of these films' surfaces.

However, beyond this seemingly similar surface-modification behavior, significant differences are observed for these two

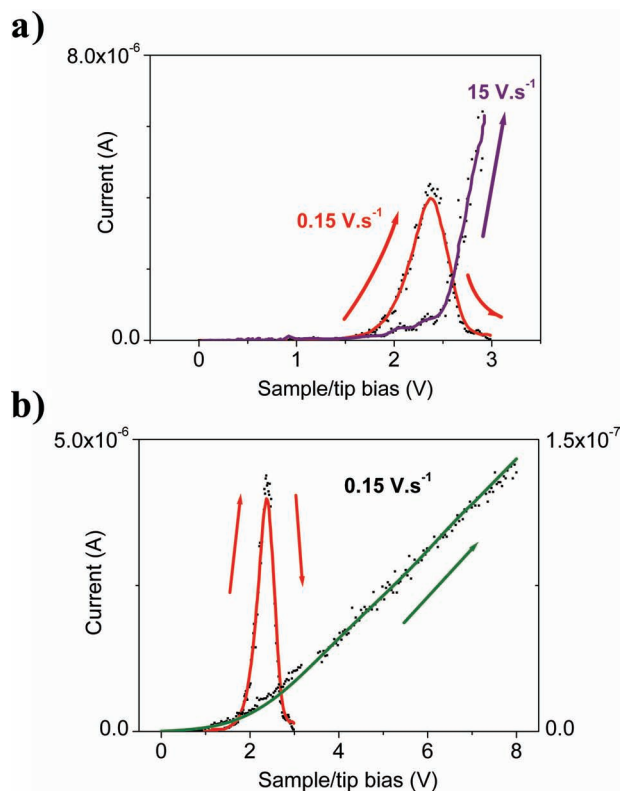


Figure 2. a) Sample/tip I - V curves of Na_xCoO_2 single crystals, using two different bias sweep rates (0.15 V s^{-1} in red and 15 V s^{-1} in purple). b) Sample/tip I - V curves of a Na_xCoO_2 single crystal (in red), and of Li_xCoO_2 thin films (in green), with the same sweep rate (0.15 V s^{-1}).

materials' probe/sample current-voltage (I - V) curves (Figure 2). For Na_xCoO_2 the shapes of the I - V curves shown in Figure 2a, depend dramatically on the potential scan rates in the positive potential range. The curve involving the slower scan rate ($V = 0.15 \text{ V s}^{-1}$) exhibits a maximum at around +2.5 V followed by a sharp decrease in the current, as a result of irreversible damage to these solids (see Supporting Information in Schneegans et al.^[5]). On the other hand, the curve obtained at higher scan rates ($V = 15 \text{ V s}^{-1}$) is free of such a current decrease: irreversible damage of the material is avoided even for potentials higher than +2.5 V. The higher scan rates correspond to shorter polarization periods and consequently to smaller amounts of locally injected faradaic charges, as in the case of the pulse mediated runs (5 ms) illustrated in Figure 1. In contrast, the I - V curves for Li_xCoO_2 thin films display (Figure 2b) a continuous increase up to +8 V, free of any irreversible modification in this potential (0 to +8 V) and scan rate range ($V = 0.15 \text{ V s}^{-1}$).

We have previously demonstrated that the faradaic currents are exceedingly low compared to the total current flowing in the probe contact-junction for the CP-AFM mediated surface-conductivity modifications.^[6] Consequently, this total current reflects unambiguously an estimation of the surface conductivity of the considered material by CP-AFM. The investigation of the current/potential curves might, therefore, allow a qualitative insight into the kinetic aspects of the processes involving these two alkali-metal intercalation-based mixed conductors,

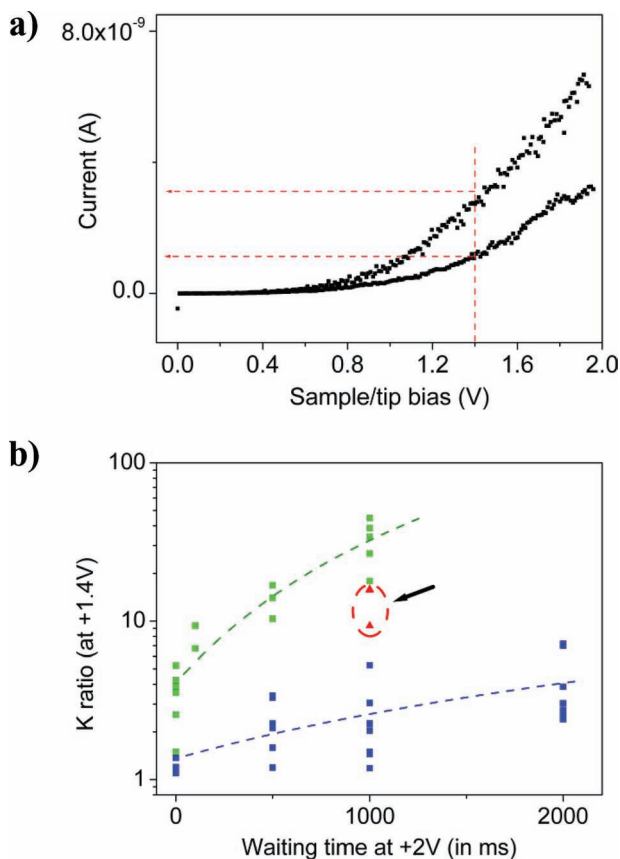


Figure 3. A qualitative insight into the CP-AFM mediated modification-kinetics of Na_xCoO₂ single crystals compared to Li_xCoO₂ thin films; a) methodology illustration: for increasing and decreasing V, *I*-*V* curves (including a 2 s waiting time at +2 V) are recorded, and a parameter K, correlated to the conductivity increase of the material, is defined as the ratio of the currents (estimated at +1.4 V) between the decreasing and increasing branches; b) the evolution of the parameter K for Na_xCoO₂ single crystals (green), as compared to Li_xCoO₂ thin films (blue), as a function of the waiting time (at +2 V); the arrow indicates the K parameter obtained at +6 V, for the Li_xCoO₂ thin films.

although the comparison involves single crystal data and polycrystalline film behavior. Considering for this purpose the 0 to +2 V potential range, the probe/substrate bias was first rapidly swept to +2 V (100 ms) and maintained at this value for a fixed period of time, and then subsequently rapidly swept back (100 ms) to 0 V. For Li_xCoO₂, this procedure yields the current/potential curve shown in Figure 3a, highlighting the increase in the total current (the increase in the surface conductivity of the solid), primarily resulting from the waiting-time period at +2 V. This increase in conductivity might be estimated (at, for example, +1.4 V) by the ratio of the currents measured for the upward and downward voltage sweeps. Using this procedure for Na_xCoO₂ single crystal and Li_xCoO₂ thin films, the corresponding results are summarized in Figure 3b. As the figure shows, the conductivity increase is significantly higher for Na_xCoO₂ than for Li_xCoO₂, at this probe/substrate bias (+2 V). The sodium diffusion-coefficients in these layered oxides ($1 \times 10^{-7} \text{ cm}^2 \text{ s}^{-1}$)^[7] are appreciably higher than those of lithium ($1 \times 10^{-10} \text{ cm}^2 \text{ s}^{-1}$)^[8] and this might account for such a behavior.

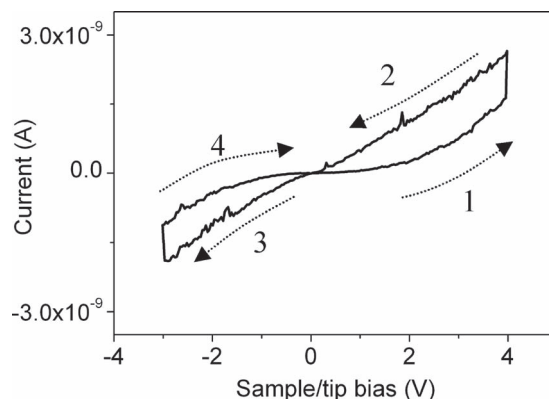


Figure 4. Sample/tip *I*-*V* curve of a Li_xCoO₂ thin film recorded by CP-AFM (sweeping rate 20 V s^{-1}) exhibiting “eightwise” switching polarity (waiting-time periods of 3 s at +4 and -3 V are established during the potential sweeps). See Supporting Information Figure 3 for a sample/tip *I*-*V* curve involving no waiting time.

However, it is interesting to note that if a higher bias (+6 V) is used for Li_xCoO₂ (green dots in Figure 3b) the corresponding increase of conductivity approaches the values obtained for Na_xCoO₂ (at +2 V).

Scanning Li_xCoO₂ over both positive and negative potential ranges, i.e., reflecting the surface-conductivity modifications illustrated in Figure 1, yields the *I*-*V* curve involving a hysteresis feature shown in Figure 4. Or, in other words, compared to the pristine-film resistance, sweeping the voltage to opposite polarities switches the probe/sample contact resistance alternately to higher or lower values. This behavior is evocative of characteristic *I*-*V* curves for bipolar resistive switching in oxide thin films,^[1,2,4] the corresponding switching polarity being “eightwise”, according to the currently used^[9] switching-polarity specific designation.^[4b] At this stage, we speculate that, beyond the surface modifications generated by the CP-AFM probe, Li_xCoO₂ might give rise to resistive switching phenomena if integrated into actual thin-film MIM devices.

A typical *I*-*V* curve of an Au/Li_xCoO₂/(p++) silicon stack, shown in Figure 5, highlights the spectacular resistive switching behavior of this MIM device, although the switching polarity is now surprisingly “counter-eightwise”. Starting at 0 V and sweeping to -4 V switches the resistance from the (pristine) high resistance state (HRS) to a low resistance state (LRS). Going back to 0 V and subsequently to +4 V switches the device back to the HRS, the cycle being then completed to 0 V. The switching is reversible over successive scans (see Supporting Information), and the ratio of the HRS to LRS is larger than in Figure 4 (four to five orders of magnitude, comparable to the ratio of the conductivity modifications of the Li_xCoO₂ observed as a function of *x*).^[10]

This interesting bipolar switching behavior, observed in this distinct category of materials, involves for the first time alkali-metal ion movements within a layered cobalt oxide lattice, in contrast with previous studies typically involving oxygen-vacancy migrations along lattice dislocations.^[4a,c] The latter generate the formation (and disruption) of conducting channels, and usually require an initial “electroforming” step^[11] not

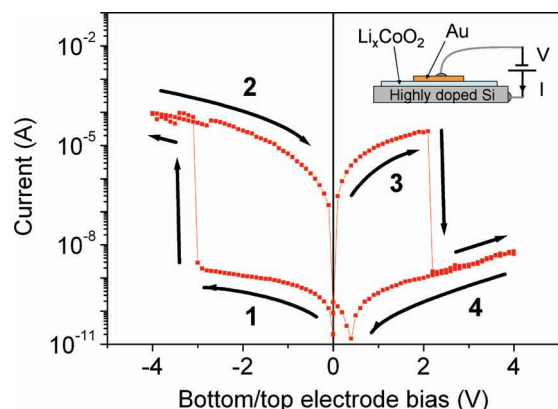


Figure 5. The I - V characteristics of the MIM device made from a Li_xCoO_2 thin film (schematicized in the upper left insert) exhibiting a resistive-switching behavior (the sweeping rate of the potential, from 0 to -4 V, back to $+4$ V, and ultimately to 0 V, is 100 mV s^{-1}). A very rapid switching from HRS to LRS occurring at about -3 V is shown (the HRS is then maintained while sweeping the potential from $+3$ to $+4$ V and back to 0 V); sweeping the potential to the opposite polarity shows an abrupt switching of the LRS to the HRS around $+2.5$ V (the latter is maintained when sweeping the potential from $+2.5$ to $+4$ V and back to 0 V).

needed in our present material. CP-AFM has proved a powerful means to investigate previous thin-film memresistive devices involving such filamentary current distributions at the origin of the earlier switching process.^[12] In contrast, the well-known conductivity of the presently investigated mixed conductor, currently used on large scales in lithium-ion rechargeable batteries, undoubtedly involves a bulk “homogeneous” process rather than a localized filamentary one. On the other hand, the results of these preliminary investigations of the MIM device, at present, leave open questions about the nature of the exact mechanisms of the process involved: for instance, i) the occurrence of interfacial (electrode/oxide) conductivity modifications vs. bulk electronic changes within the devices, ii) the significance of non-equivalent interfaces within the MIM (Au/ Li_xCoO_2 vs. (p++) silicon/ Li_xCoO_2), possibly implying a specific involvement of the silicon interface, and iii) a substitute for the electrochemical processes involving an ambient-air water-condensation meniscus,^[6] put forward in the case of the CP-AFM probe-mediated local modifications. These aspects, as well as investigations of the kinetic aspect of the MIM switching associated with the downscaling of the devices are presently being actively investigated.

In conclusion, we have shown that local conductivity modifications in Li_xCoO_2 thin films are obtained by scanning the surface with a CP-AFM probe, similar to the process previously investigated in Na_xCoO_2 single crystals. The comparison of the I - V curves of these thin films with those of bipolar resistive switching in various oxide thin films suggests the possibility of obtaining a resistive switching phenomenon in Li_xCoO_2 within an actual thin-film MIM device, not yet observed with such mixed conductors. A substantial resistive switching of the device is in fact observed with this material; therefore, the previously well-known charge-storage ability of these layered-oxide conductors, used as cathode materials in rechargeable

batteries, is now combined with a possible reversible conductivity switching in these thin-films.

Experimental Section

Li_xCoO_2 thin films were fabricated: i) on a (p++) doped silicon-wafer substrate by RF magnetron reactive sputtering (Alcatel SCM 600 apparatus) using a stoichiometric ($x = 1$) Li_xCoO_2 target, with an applied RF power of 500 W. The films were grown in a 3/1 Ar/ O_2 (2.2 Pa) atmosphere and a bias of -50 V was applied to the substrate. The films (100 nm, as determined by a profilometer) were subsequently heated to 600 °C for 1 h in air in order to obtain the crystallized $R\text{-}3m$ high-temperature Li_xCoO_2 phase. The corresponding stoichiometry was determined by atomic absorption spectroscopy and X-ray diffraction (XRD) experiments to be $x = 0.9$. ii) On (0001) Al_2O_3 substrates using a stoichiometric LiCoO_2 target, the sapphire substrates were annealed in air at 1100 °C for 5 h in order to obtain an ultra smooth surface. The ablation of the target was carried out in a vacuum chamber using a KrF laser (COMPexPro 201, $\lambda = 248$ nm and $\tau = 25$ ns) operated at 1 Hz with a fluence of $\approx 1.3 \text{ J cm}^{-2}$. During the deposition the oxygen pressure in the chamber was kept at 100 Pa and the substrate was maintained at the deposition temperature of 400 °C. The stoichiometry of the resulting films, determined by XRD (θ - 2θ scan mode) was $x = 0.78$.

Na_xCoO_2 single crystal preparation and CP-AFM instrumentation have been previously described.^[5]

The MIM devices were obtained by the deposition of upper Au electrodes on the Li_xCoO_2 thin films by conventional Joule evaporation; rectangular pads of around $100 \times 400 \mu\text{m}^2$ were used to characterize the switching properties. I - V measurements were performed under vacuum (5×10^{-6} Torr) using a Keithley K487 instrument as both a voltage source and current ammeter.

Supporting Information

Supporting Information is available from the Wiley Online Library or from the author.

Acknowledgements

Financial support from DGES-C’Nano Idf (Monaco project) is gratefully acknowledged.

Received: May 13, 2011

Published online: August 5, 2011

- [1] F. Argall, *Solid-State Electron.* **1968**, *11*, 535.
- [2] a) D. B. Strukov, G. S. Snider, D. R. Stewart, R. S. Williams, *Nature* **2008**, *453*, 80; b) R. S. Williams, *IETE Tech. Rev.* **2010**, *27*, 181.
- [3] a) R. Waser, R. Dittmann, G. Staikov, K. Szot, *Adv. Mater.* **2009**, *21*, 2632; b) R. Waser, M. Aono, *Nat. Mater.* **2007**, *6*, 833.
- [4] a) J. P. Strachan, M. D. Pickett, J. J. Yang, S. Aloni, A. L. D. Kilcoyne, G. Medeiros-Ribeiro, R. S. Williams, *Adv. Mater.* **2010**, *22*, 3573; b) R. Muenstermann, T. Menke, R. Dittmann, R. Waser, *Adv. Mater.* **2010**, *22*, 4819; c) D.-H. Kwon, K. M. Kim, J. H. Yang, J. M. Jeon, M. H. Lee, G. H. Kim, X.-S. Li, G.-S. Park, B. Lee, S. Han, M. Kim, C. S. Hwang, *Nat. Nanotechnol.* **2010**, *5*, 148; d) H. Y. Jeong, J. Y. Lee, S.-Y. Choi, J. W. Kim, *Appl. Phys. Lett.* **2009**, *95*, 162108; e) D. S. Jeong, H. Schroeder, R. Waser, *Phys. Rev. B* **2009**, *79*, 195317; f) M. D. Pickett, D. B. Strukov, J. L. Borghetti, J. J. Yang, G. S. Snider, D. R. Stewart, R. S. Williams, *J. Appl. Phys.* **2009**, *106*, 074508; g) D. S. Jeong, H. Schroeder, R. Waser, *Electrochem. Solid-State Lett.* **2007**, *10*, G51.

- [5] O. Schneegans, A. Moradpour, O. Dragos, S. Franger, N. Drago, L. Pinsard-Gaudart, P. Chretien, A. Revcolevschi, *J. Am. Chem. Soc.* **2007**, *129*, 7482.
- [6] O. Schneegans, A. Moradpour, L. Boyer, D. Ballutaud, *J. Phys. Chem. B* **2004**, *108*, 9882.
- [7] G. J. Shu, F. C. Chou, *Phys. Rev. B* **2008**, *78*, 052101.
- [8] Q. Cao, H. P. Zhang, G. J. Wang, Q. Xia, Y. P. Wu, H. Q. Wu, *Electrochem. Commun.* **2007**, *9*, 1228.
- [9] a) X. Gao, Y. Xia, J. Ji, H. Xu, Y. Su, H. Li, C. Yang, H. Guo, J. Yin, Z. Liu, *Appl. Phys. Lett.* **2010**, *97*, 193501; b) K. Shibuya, R. Dittmann, S. Mi, R. Waser, *Adv. Mater.* **2010**, *22*, 411.
- [10] M. Ménétrier, I. Saadoune, S. Levasseur, C. Delmas, *J. Mater. Chem.* **1999**, *9*, 1135.
- [11] a) D. S. Jeong, H. Schroeder, R. Waser, *Nanotechnology* **2009**, *20*, 375201; b) J. J. Yang, F. Miao, M. D. Pickett, D. A. A. Ohlberg, D. R. Stewart, C. N. Lau, R. S. Williams, *Nanotechnology* **2009**, *20*, 215201; c) C. Nauenheim, C. Kuegeler, A. Ruediger, R. Waser, *Appl. Phys. Lett.* **2010**, *96*, 122902; d) K. M. Kim, G. H. Kim, S. J. Song, J. Y. Seok, M. H. Lee, J. H. Yoon, C. S. Hwang, *Nanotechnology* **2010**, *21*, 305203.
- [12] a) K. Szot, W. Speier, G. Bihlmayer, R. Waser, *Nat. Mater.* **2006**, *5*, 312; b) K. Szot, R. Dittmann, W. Speier, R. Waser, *Phys. Status Solidi RRL* **2007**, *1*, R86.